Crystallization kinetics and network rigidity

2008 J. Phys.: Condens. Matter 20 335203

(http://iopscience.iop.org/0953-8984/20/33/335203)

IOP PUBLISHING JOURNAL OF PHYSICS: CONDENSED MATTER

J. Phys.: Condens. Matter **20** (2008) 335203 (4pp) doi:10.1088/0953-8984/20/33/335203

Crystallization kinetics and network rigidity

Isak Avramov[1], Christian Rüssel[2], Natalia Kolkovska[3] and Ivan Georgiev[3]

[1] Institute of Physical Chemistry, Bulgarian Academy of Science, Academician Georgi Bonchev Street, building 11, 1113, Sofia, Bulgaria
[2] Otto Schott Institut, Friedrich-Schiller- University, Fraunhoferstraße 6, D-07743, Jena, Germany
[3] Institute of Mathematics and Informatics, Bulgarian Academy of Science, Academician Georgi Bonchev Street, building 8, 1113, Sofia, Bulgaria

E-mail: avramov@ipc.bas.bg, ccr@rz.uni-jena.de, natali@math.bas.bg and john@parallel.bas.bg

Received 1 April 2008, in final form 2 June 2008
Published 21 July 2008
Online at stacks.iop.org/JPhysCM/20/335203

Abstract

Kinetics of crystal growth in non-isochemical systems is considered taking into account the changes in composition of the residual melt during the process. This leads to the formation of concentration gradients in the vicinity of the new phase. If a component acting as a network modifier is enriched in the crystalline phase, the melt at the interface is enriched in network formers and the glass network will turn from floppy to rigid. Consequently, the crystal grows until a critical concentration is reached, at which the melt locally turns to a rigid one. There is a critical size of the crystal, above which the growth rate strongly decreases because the network former concentration at the interface drops below the threshold limit. The problem is solved numerically and finite differences are used for space and time discretization.

(Some figures in this article are in colour only in the electronic version)

1. Introduction

For nucleation and crystal growth, the chemical composition and hence the structure of the liquid is decisive. This is of particular importance for multicomponent systems, i.e. liquids which have a composition different from that of the nucleus formed. In highly viscous melts, near the glass transition temperatures, this leads to a formation of diffusion layers (diffusion of stress deformation energy as well as diffusion of chemical components) at the crystal surface. Here, two cases can be distinguished: (i) the viscosity of the liquid at the interface is lower than that in the bulk; this leads to an increase in the crystal growth velocity due to enhanced mobility. If, however, (ii) the viscosity increases, the interface will act as a barrier and will notably decelerate the crystal growth velocity.

Recently a new approach was suggested: the combination of the percolation theory and the classical nucleation theory [1–4]. Most of the glass-forming systems are well described by the continuous-random-network model of Zachariasen [5]. Finney and Bernal [6] describe the glass structure by means of Voronoi polyhedra. Gupta and Cooper [7] used distorted polytypes to describe the structure of glass-forming melts. The concept of average coordination number $\langle r \rangle$ is an important logical step in this line. According to Mott [8], the coordination number of covalently bonded atoms is determined by the number of outer shell electrons. It can be connected with the constraint counting concepts of Phillips [9, 10] and Thorpe [11–13]. It was shown in [12] that the network becomes rigid if the mean coordination of network formers $\langle r \rangle$ exceeds a critical value $r_c \geqslant 2.4$.

The main idea of the present article is to simulate the crystal growth in multicomponent systems with crystal composition different from that of the ambient phase. Anticipating, we expect an initial stage of diffusion controlled growth followed by a second stage of much slower growth due to the switch from floppy to rigid of the melt in the crystal vicinity.

2. Mathematical formulation

We consider a half-line domain $0 < z < \infty$ full of material, which at each time and each point is in one of the following two states: crystalline and melt. The special point is the change in the diffusion coefficient caused by the switch of the liquid network from 'floppy' to 'rigid' as the concentration of modifying ions drops below a critical value C_{cr}. The interface between the crystal and liquid phase, given by the curve $\xi(t)$, is denoted by $\Gamma(t)$. The region where the crystal grows is $0 < z < \xi(t)$. We suppose that the concentration of network modifying components in the crystal is fixed, $C_{\mathrm{c}} = 1$.

In the following, the dependence of the concentrations $C(z, t)$ in the melt at the distance z and time t is considered. According to Fick's law, it is given by the equation

$$\frac{\partial C(z,t)}{\partial t} = \frac{\partial}{\partial z}\left(D\,(C)\,\frac{\partial C(z,t)}{\partial z}\right), \qquad \xi(t) < z < \infty. \tag{1}$$

Note that the diffusion coefficient D is piecewise constant—at the critical concentration C_{cr} the properties of the network change and the coefficient D switches from $D^{(1)}$ to $D^{(2)}$. On the interface $\Gamma(t)$ between crystal and melt the following jump condition holds:

$$\frac{\partial \xi(t)}{\partial t} = D\,(C)\,\frac{\partial C(\xi(t),t)}{\partial z}. \tag{2}$$

Equation (2) is commonly referred to as the Stefan condition. For the classical Stefan problem one sets a fixed concentration on $\Gamma(t)$, but for our application we take into account the concentration transport from the melt into the crystalline phase. Thus the second boundary condition on the interface $\Gamma(t)$ is

$$D\,(C)\,\frac{\partial C(\xi(t),t)}{\partial z} = \frac{W}{d_0}(C(\xi(t),t) - C_{\mathrm{e}}). \tag{3}$$

Here W is a dimensionless constant, d_0 is the intermolecular distance and C_{e} is the equilibrium concentration at the crystal/melt interface. We set $K = W/d_0$. The initial concentration is given by

$$C(z,0) = C_{\mathrm{in}}, \qquad C_{\mathrm{in}} = C_\infty \tag{4}$$

and for $z \to \infty$ we have

$$\lim_{z\to\infty} C(z,t) = C_\infty. \tag{5}$$

The crystallization process starts at time $t = 0$, thus $\xi(0) = 0$.

Problem (1)–(5) is a special case of moving boundary problems. In this case the boundary of the domain $\Gamma(t)$ is not known in advance. Thus the solution of the system (1)–(5) requires solution of the diffusion equations in an unknown region, which has to be determined as a part of the solution. There are very limited analytical solutions to moving boundary problems. Therefore, the numerical solution of (1)–(5) is the main tool in the study of these problems.

Various numerical methods are known to solve Stefan type problems, e.g. front-fixing method, front-tracking method, level-set method, phase field method. For a comparison of several effective methods for the one-dimensional Stefan problem see [14, 16]. We apply the boundary immobilization method [14, 15]. In this method the domain of the melt phase is transformed into a fixed one at the expense of solving a more complicated equation (compare (1) and (6)). The benefit is that only a little additional effort is required to treat the moving boundary. Moreover, the new form of the equations is suited to standard numerical procedures.

3. Description of the numerical algorithm

In this section we explain our numerical method. First, we reformulate the problem using the transformation

$$x = z - \xi(t), \qquad c(x,t) = C(z,t).$$

Under this transformation, the domain of the melt phase is mapped onto the fixed one $\{0 < x < \infty, 0 < t\}$ with unknown functions c and ξ. In the new coordinate system x, t equations (1)–(3) take the form

$$\frac{\partial c(x,t)}{\partial t} = \frac{\partial}{\partial x}\left(D(c)\frac{\partial c(x,t)}{\partial x}\right) + \frac{\partial \xi(t)}{\partial t}\frac{\partial c(x,t)}{\partial x}, \quad 0 < x < \infty, \tag{6}$$

$$D(c)\frac{\partial c(0,t)}{\partial x} = K(c(0,t) - C_{\mathrm{e}}), \quad \lim_{x\to\infty} c(x,t) = C_\infty, \tag{7}$$

$$\frac{\partial \xi(t)}{\partial t} = K(c(0,t) - C_{\mathrm{e}}). \tag{8}$$

Further, we fix a sufficiently large interval $[0, x_\infty]$ and introduce the non-uniform grid $\{x_k\}, k = 0, 1, \ldots, N$, $x_0 = 0, x_N = x_\infty$ on it with step-sizes $h_k = x_k - x_{k-1}$. The grid $\{x_k\}$ is concentrated at 0. The time grid $\{t_j\}$ is uniform with step τ.

We define discrete approximations $c(x_k, t_j)$ to the concentration at the point x_k at time t_j and approximations $\xi(t_j)$ to the position of the front at the time moment t_j. Suppose that at the moment t_{j-1} the concentration $c(x_k, t_{j-1})$ and the position $\xi(t_{j-1})$ of the front are known. At the next time $t_j = t_{j-1} + \tau$ we have to compute the new position of the front $\xi(t_j)$ and the concentration $c(x_k, t_j)$.

The discretization of equations (6)–(8) using the central difference for the convection term and a standard six-point finite difference scheme with parameter $\sigma \in [0, 1]$ (see for example [17]) is in the form

$$\begin{aligned}
&\frac{c(x_k,t_j) - c(x_k,t_{j-1})}{\tau} \\
&= \sigma\frac{2D(c(x_k,t_j))}{h_k + h_{k+1}}\frac{c(x_{k+1},t_j) - c(x_k,t_j)}{h_{k+1}} \\
&\quad - \sigma\frac{2D(c(x_k,t_j))}{h_k + h_{k+1}}\frac{c(x_k,t_j) - c(x_{k-1},t_j)}{h_k} \\
&\quad + (1-\sigma)\frac{2D(c(x_k,t_{j-1}))}{h_k + h_{k+1}}\frac{c(x_{k+1},t_{j-1}) - c(x_k,t_{j-1})}{h_{k+1}} \\
&\quad - (1-\sigma)\frac{2D(c(x_k,t_{j-1}))}{h_k + h_{k+1}}\frac{c(x_k,t_{j-1}) - c(x_{k-1},t_{j-1})}{h_k} \\
&\quad + \frac{\xi(t_j) - \xi(t_{j-1})}{\tau}\sigma\frac{2}{h_k + h_{k+1}}\left(c(x_{k+1},t_j) - c(x_{k-1},t_j)\right)
\end{aligned}$$

$$+\frac{\xi(t_j)-\xi(t_{j-1})}{\tau}(1-\sigma)\frac{2}{h_k+h_{k+1}}(c(x_{k+1},t_{j-1}) - c(x_{k-1},t_{j-1})), \tag{9}$$

for $k = 1, 2, \ldots, N-1$ and

$$\frac{c(0,t_j)-c(0,t_{j-1})}{\tau} = \sigma\frac{2}{h_1}\frac{D(c(0,t_j))(c(x_1,t_j)-c(0,t_j))}{h_1} - \sigma\frac{2}{h_1}K\left(1-0.5h_1\frac{\xi(t_j)-\xi(t_{j-1})}{D(c(0,t_j))\tau}\right)\left(c(0,t_j)-C_e\right) + (1-\sigma)\frac{2}{h_1}\frac{D(c(0,t_j))(c(x_1,t_{j-1})-c(0,t_{j-1}))}{h_1} - (1-\sigma)\frac{2}{h_1}K\left(1-0.5h_1\frac{\xi(t_j)-\xi(t_{j-1})}{D(c(0,t_j))\tau}\right) \times \left(c(0,t_{j-1})-C_e\right), \tag{10}$$

for $k = 0$.

Finally, we use the equation

$$\frac{\xi(t_j)-\xi(t_{j-1})}{\tau} = K\left(\sigma c(0,t_j)+(1-\sigma)c(0,t_{j-1})-C_e\right) \tag{11}$$

for the approximation of the front position at the next moment of time.

Note that the accuracy of the numerical method is first order in time and second order in space for $\sigma \neq 0.5$. The scheme with $\sigma = 0.5$ can be used to achieve second order accuracy both in space and in time. In the case of explicit discretization ($\sigma = 0$) the time step stability restriction

$$\tau \leqslant \frac{\min(h_i)^2}{4\max(D, K\max h_i)}$$

is needed (see [17]). Implicit time discretization $\sigma > 0$ avoids the time step stability restriction.

The additional step restrictions

$$\tau \leqslant \frac{\min(h_i)^2}{2D(1-\sigma)}, \qquad h \leqslant \frac{2D(c)}{K(c(0,t_j)-C_e)}$$

are sufficient for the positivity and the monotonicity of the numerical solution.

Thus, we obtain a non-linear system of equations (9)–(11) for $c(x_k, t_j)$ and $\xi(t_j)$. This system is solved iteratively. The initial value $\xi^0(t_j)$ of $\xi(t_j)$ is obtained from (11) with $\sigma = 0$. The iteration step is the computation of the concentrations $c(x_k, t_j)$, $k = 0, 1, \ldots, N$, from equations (9) and (10). Equation (11) with $\sigma = 0.5$ and the already evaluated concentration $c(0, t_j)$ gives the next iteration $\xi^1(t_j)$ of the front position. Iterations continue until $|\xi^m(t_j) - \xi^{m-1}(t_j)| < \epsilon$, where ϵ is a given precision.

The resulting linear algebraic system (for $\sigma \neq 0$) is non-symmetric and tridiagonal. It is diagonally dominant with positive diagonal entries and non-positive off-diagonal elements. Therefore, we can apply fast linear solvers to compute the concentrations—for example the Thomas algorithm.

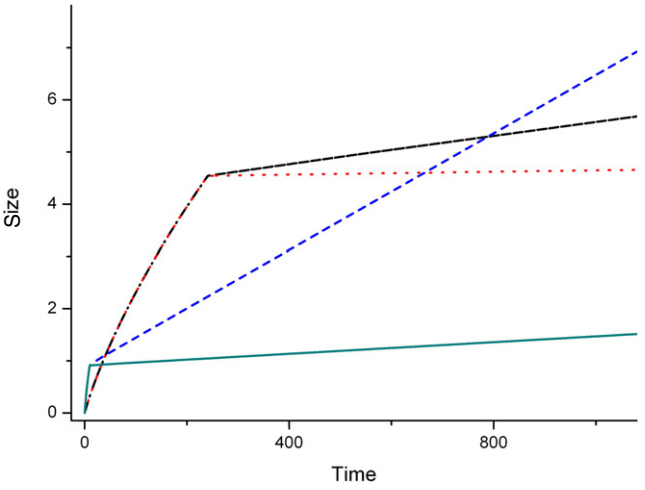

Figure 1. Crystal size.

4. Results and discussion

We consider equations (1)–(5) with the following physical parameters:

$$D^{(1)} = 1, \qquad D^{(2)} = \frac{D^{(1)}}{a}, \quad \text{where } a = 10 \text{ or } a = 100,$$
$$W = 0.5 \text{ or } W = 0.1, \qquad C_{in} = C_\infty = 0.7, \qquad C_e = 0.3, \qquad C_{cr} = 0.44. \tag{12}$$

For the numerical solution of equations (1)–(5) with physical parameters (12) we use the above described algorithm with parameter $\sigma = 0$.

Figure 1 shows the time dependence of the size of the growing crystal. The solid line is for $a = 100$ and $W = 0.5$; the dashed line is for $a = 10$ and $W = 0.5$; the dotted line is for $a = 100$ and $W = 0.1$ and dash–dotted line is for $a = 10$ and $W = 0.1$. A clear break in the growth rate is seen. Initial fast growth switches to slower growth as soon as the concentration at the interface drops below the critical value. Two important peculiarities are seen. For $W = 0.1$ the initial growth rate is about five times slower, as expected. The initial mode of growth lasts longer because the concentration is not consumed so fast and the diffusion supply keeps the interface concentration sufficiently high for a longer time. Moreover, the thickness of the rigid shell with $C < C_{cr}$ remains thinner. At the first site the final result is quite paradoxical: lowering the W value causes an increase of the growth rate.

The time dependence of the size of the 'rigid shell', the zone with lowered diffusion coefficient in the interface region, is demonstrated in figure 2. The upper part of the same figure illustrates the time dependence of the concentration at the interface. The starting point is the moment when the 'rigid shell' is first formed. In order to see better the initial stages, the time is shown in a log scale. The thickness n increases stepwise. It is readily seen that it is correlated with the concentration decrease at the interface.

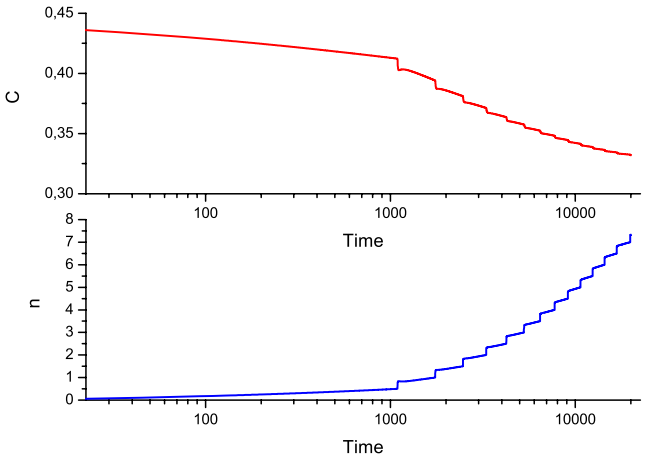

Figure 2. Size of the rigid shell and concentration at the interface.

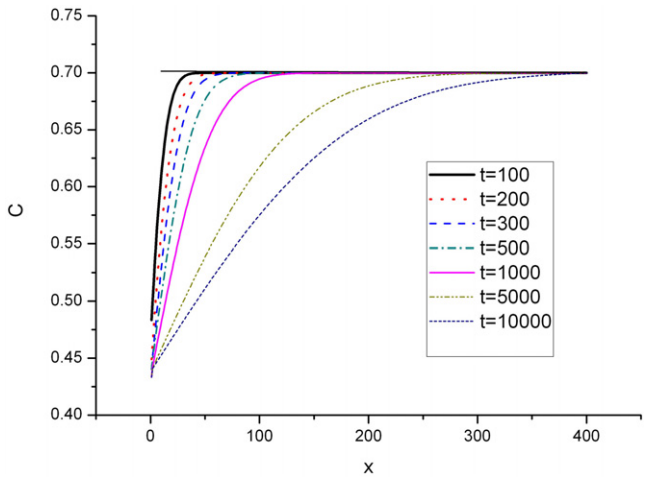

Figure 3. Concentration profiles.

The 'rigid shell' grows faster if $a = 10$ in comparison to $a = 100$. This is because diffusion supplies the 'rigid shell' from outside with network modifiers, i.e. the same material that is consumed by the growing crystal. In the same time the consumption is slower for $a = 100$.

Figure 3 demonstrates the concentration profiles at different times. The initial stage is a straight line, $C = C_{\text{in}}$. The time is indicated on each curve. As soon as the growth begins a diffusion zone is formed.

The concentration at the interface, i.e. $x = 0$, drops very fast, long before a steady state is approached. In the particular case in figure 2, the concentration at the interface is below the critical point of $C = C_{\text{cr}}$ even for $t = 100$, though for the time $t = 10\,000$ it is far from steady state conditions.

5. Conclusions

A 'rigid' shell is formed near the interface of the growing crystal. The reason is the exhaustion of concentration of modifying components in this region. This is in agreement with data of [18], who find experimentally about a 30 nm rigid region in the vicinity of the newly formed crystals.

As a result of the formation of the 'rigid' shell the mode of growth changes and the crystals almost stop growing.

Acknowledgment

Financial support from the EU Project INTERCONY, contract no NMP4-CT-2006-033200, is appreciated.

References

[1] Avramov I, Keding R and Rüssel C 2000 *J. Non-Cryst. Solids* **272** 147
[2] Avramov I, Keding R, Rüssel C and Kranold R 2000 *J. Non-Cryst. Solids* **278** 13
[3] Avramov I, Keding R and Rüssel C 2000 *Glastech. Ber. Glass Sci. Technol.* **73 C1** 138
[4] Keding R and Rüssel C 2005 *J. Non-Cryst. Solids* **351** 1441
[5] Zachariasen W 1932 *J. Am. Chem. Soc.* **54** 3841
[6] Finney G and Bernal J 1967 *Nature* **213** 1079
[7] Gupta P and Cooper A 1992 *Proc. 16th Int. Congress on Glass (Madrid: Bol. Sociedad Espagniola de Ceram. Vidio 31c)* p 15
[8] Mott N 1969 *Phil. Mag.* **19** 835
[9] Phillips J and Thorpe M 1986 *Solid State Commun.* **53** 84
[10] Phillips J 1979 *J. Non-Cryst. Solids* **73** 153
[11] Thorpe M 1983 *J. Non-Cryst. Solids* **57** 355
[12] Thorpe M 1989 *Phys. Rev.* B **40** 535
[13] Thorpe M 1995 *J. Non-Cryst. Solids* **182** 135
[14] Caldwell J and Kwan Y 2004 *Commun. Numer. Methods Eng.* **20** 535
[15] Crank J 1975 *The Mathematics of Diffusion* (Oxford: Clarendon)
[16] Javierre E, Vuik C, Vermolen F and Zwaag S 2006 *J. Comput. Appl. Math.* **192** 445
[17] Paskonov V M, Polejaev V I and Tchudov L A 1984 *The Numerical Modeling of Processes of Heat and Mass Transfer* (Moscow: Nauka) (in Russian)
[18] Rüssel C 2005 *Chem. Mater.* **17** 5843